Sonographic Findings of Axillary Masses

What Can Be Imaged in This Space?

Ji Eun Park, MD, Yu-Mee Sohn, MD, PhD, Eun-Kyung Kim, MD, PhD

The diagnosis of axillary masses can be challenging because various tumors can develop in parts of the axilla other than lymph nodes, even though we frequently encounter axillary masses in daily practice. These lesions include soft tissue masses associated with nontumorous conditions (accessory breast tissue and chronic granulomatous inflammation) and benign and malignant tumorous conditions (lipomas, epidermal inclusion cysts, lymphangiomas, fibroadenomas, schwannomas, malignant neuroendocrine tumors, and lymph node–associated diseases). In this pictorial essay, we display commonly encountered sonographic findings of various axillary lesions to assist in the differential diagnosis of axillary masses.

Key Words—axillary masses; nontumorous conditions; sonography; tumorous conditions

Received September 7, 2012, from the Department of Radiology, Kyung Hee University Hospital, College of Medicine, Kyung Hee University, Seoul, Korea (J.E.P., Y.-M.S.); and Department of Radiology, Research Institute of Radiological Science, Yonsei University College of Medicine, Seoul, Korea (E.-K.K.). Revision requested September 25, 2012. Revised manuscript accepted for publication November 8, 2012.

Address correspondence to Yu-Mee Sohn, MD, PhD, Department of Radiology, Kyung Hee University Hospital, College of Medicine, Kyung Hee University, 23 Kyungheedae-ro, Dongdaemun-gu, Seoul 130-872, Korea.

E-mail: sonyumee@naver.com

Abbreviations
CT, computed tomography

doi:10.7863/ultra.32.7.1261

The axilla is a triangular space between the upper portion of the arm and the lateral side of the thorax. Its apex is directed toward the neck, and its base is directed downward. The axilla contains arteries, veins, lymph nodes, the long thoracic and intercostobrachial nerves, axillary fat, and areolar tissue, all of which can develop various diseases.[1–3] The clinical features of axillary lesions are frequently palpable axillary masses, pain, and arm swelling.[2] The most commonly reported palpable axillary masses are metastatic lymph nodes associated with breast cancer.[4] However, because the axilla contains various tissues, the differential diagnosis of an axillary mass includes axillary parenchymal lesions as well as lymph nodes.[3] The purpose of this pictorial essay is to review the sonographic findings of various axillary masses that were confirmed cytopathologically or by pathognomonic findings on images to help in the differential diagnosis of axillary masses.

Nontumorous Conditions of the Axilla

Accessory Breast Tissue

The development of mammary tissue in the human embryo begins at 5 weeks' gestation. The ectodermal primitive milk line and galactic band develop from the axilla to the groin bilaterally. At 7 weeks' gestation, the band develops to form a mammary ridge in the thorax, eventually becoming the mammary glands. The remaining primitive milk line generally regresses.[4,5] Accessory breast tissue is caused by a failure of the primitive mammary tissue to regress.[6] This tissue can occur anywhere along the primitive embryonic milk lines, which extend from the axilla to the groin, and it may occur unilaterally or bilaterally. The axilla is the most commonly involved site of accessory breast tissue, followed by the inframammary area. Accessory breast tissue is found in 2% to 6 % of women. It may enlarge during pregnancy or lactation because of its sensitivity to estrogen, and its size can change during the menstrual period.[4,7] In addition, discomfort, pain, and local skin irritation can occur.[8] Sonography shows a masslike lesion and echogenic density that corresponds to that of the normal breast parenchyma (Figure 1).

Chronic Granulomatous Inflammation of Lymph Nodes

The terms *chronic lymphadenitis* and *granulomatous lymphadenitis* refer to a collection of lymph nodes with granulomatous lesions or chronic abscesses that partially or completely efface the normal nodal architecture.[9] Granulomatous lymphadenitis is seen in a wide variety of infectious and noninfectious diseases. Infectious granulomatous diseases include tuberculosis, leprosy, and cryptococcosis. Noninfectious granulomatous diseases include sarcoidosis and Crohn disease.[10] Tuberculosis is the most common cause of benign granulomatous axillary lymphadenitis.[6,9] Cervical lymph nodes are the most commonly involved peripheral lymph nodes, followed by inguinal and axillary lymph nodes.[3]

Sonography shows variable-size, irregular heterogeneous hypoechoic masses. Color Doppler sonography shows increased blood flow in the mass. Tuberculous lymphadenitis is seen as multiple enlarged conglomerated hypoechoic nodes with or without dense dystrophic calcifications (Figure 2). Associated internal necrosis (cystic areas) and surrounding fat changes are caused by inflammation. The presence of macrocalcifications frequently indicates tuberculosis.[6] Computed tomography (CT) reveals central low density and cystic changes in the lymph node, depending on the degree of caseation.[3]

Benign Tumorous Conditions

Lipomas

Lipomas are the most common mesenchymal soft tissue tumors, accounting for almost half of all soft tissue tumors.[11,12] They are benign tumors composed of mature lipocytes. Lipomas can occur in all parts of the body, including the axilla.[13] On physical examination, lipomas are usually soft painless masses.[14]

Sonography commonly shows an elliptical or ovoid well-circumscribed compressible solid lesion in the subcutaneous fatty layer with a parallel orientation to the skin layer (Figure 3A).[12,15] Its internal echogenicity is most often variable or mixed echogenicity from hypoechogenicity to hyperechogenicity, which is related to the number of internal interfaces between fat and other connective elements.[4,12,16,17]

Figure 1. Accessory breast tissue in a 31-year-old woman with a history of a left palpable axillary mass. Transverse sonography shows a heterogeneous hyperechoic area similar to normal glandular tissue just below the skin (arrows).

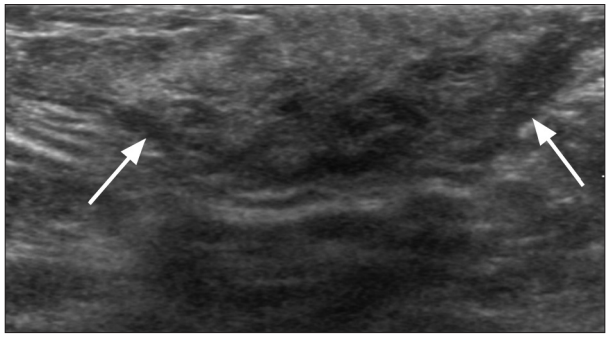

Figure 2. Tuberculous lymphadenitis in a 72-year-old woman with a history of a left palpable axillary mass. Transverse sonography shows enlarged heterogeneous hypoechoic multiple lymph nodes (arrows).

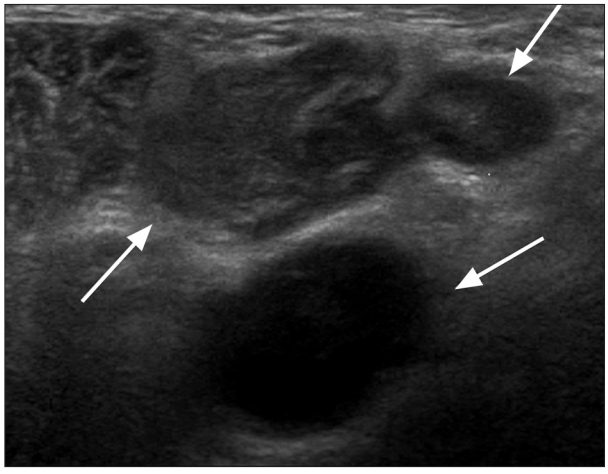

Real-time elastography shows a mass as soft as surrounding tissue with the lowest elasticity score of 1.[18] Mammography shows a low-density mass, often surrounded by a thin fibrous capsule (Figure 3B).[16] Computed tomography shows a well-defined ovoid mass with homogeneous imaging characteristics of fat.[14] The Hounsfield units on CT are typically approximately –65 to –120, similar to normal subcutaneous fat. Lipomas usually do not show any contrast enhancement on CT.[4]

Epidermal Inclusion Cysts

Epidermal inclusion cysts are benign cysts usually found on the skin. Histologically, the cyst is surrounded by a wall of stratified squamous epithelium with a granular layer.[19,20] Epidermal inclusion cysts result from occlusion of the pilosebaceous unit or implantation of variable epidermal cells in the dermis or subcutaneous area.[21,22] Various complications can occur, such as rupture and inflammation. In cases of spontaneous rupture, cysts release keratin, which acts as an irritant, leading to secondary inflammation.[4,23] Sonography shows a well-circumscribed lesion, although it may be poorly defined when associated inflammation is present (Figure 4A). The internal echogenicity varies, ranging from anechoic to more hypoechoic and heterogeneous, depending on the internal contents of the cyst. Occasionally, epidermal inclusion cysts can appear as structures with a pseudotestis appearance, with some intralesional bright echogenic reflectors and filiform

Figure 3. Lipoma in a 44-year-old woman with a history of a right palpable axillary mass. **A**, Transverse sonography shows a well-circumscribed heterogeneous isoechoic mass in the subcutaneous layer (arrows). **B**, Mammography shows a fat density mass (arrows) surrounded by a thin fibrous capsule in the right axilla with a BB marker (arrowhead) at the palpable site.

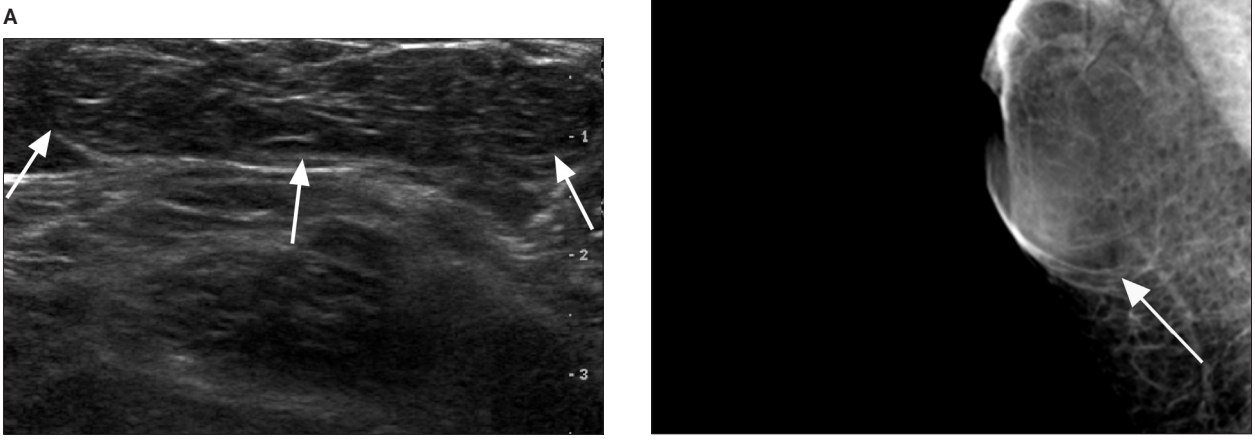

Figure 4. Infected epidermal inclusion cyst in a 34-year-old man with a history of a left palpable axillary mass. **A**, Transverse sonography shows a large heterogeneous hypoechoic mass with a lobulated contour, echogenic debris, and surrounding soft tissue edema in the subcutaneous layer (arrows). **B**, Color Doppler sonography shows increased vascularity mainly located in the periphery of the cyst (arrow).

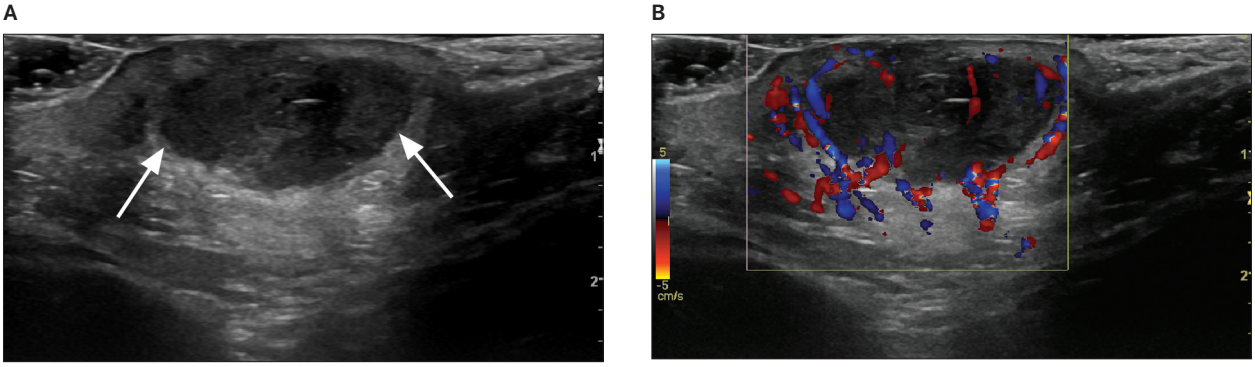

anechoic areas.[21,24] A ruptured epidermal inclusion cyst may have a lobulated shape and vascular flow in the periphery due to associated inflammation on color Doppler imaging (Figure 4B).[12,21,23,25,26]

Lymphangiomas

Most lymphangiomas are congenital malformations that arise from a primordial lymphatic system.[4] Malformation of the lymphatic system leads to failed drainage into the veins.[4,6] Lymphangiomas can occur anywhere in the mucosa and skin. The most common sites are in the neck, followed by the proximal extremities such as the axillary area.[4,6]

Sonography shows a well-defined multilocular cystic mass containing multiple septations (Figure 5A).[4,27] Color Doppler imaging shows no flow in the mass (Figure 5B).[28] Mammography shows a large and homogeneous density in the axilla.[6] Computed tomography shows a multiloculated cystic mass with enhancement in the internal septations (Figure 5C).[27]

Fibroadenomas

Fibroadenomas of the breast are relatively frequent benign tumors. On physical examination, they generally appear as well-circumscribed painless masses in women. Fibroadenomas are rarely found in accessory breast tissue in the axilla.[8]

Sonography shows a homogeneous hypoechoic lesion with a smooth contour and well-circumscribed margins (Figure 6A).[29] In rare cases, sonography shows a heterogeneous echo texture, a finding that reveals necrosis or dystrophic calcifications, which is common in older women.[29] Color Doppler imaging shows increased blood flow (Figure 6B). Mammography shows a nonspecific mass, which can present as a well-circumscribed round, oval, or lobulated isodense mass. Calcifications occasionally mimic malignant microcalcifications, but in the presence of the coarse calcifications, they are characteristically benign. Thus, further evaluation, including breast sonography or biopsy, is not needed.[4,30] Gadolinium-enhanced magnetic

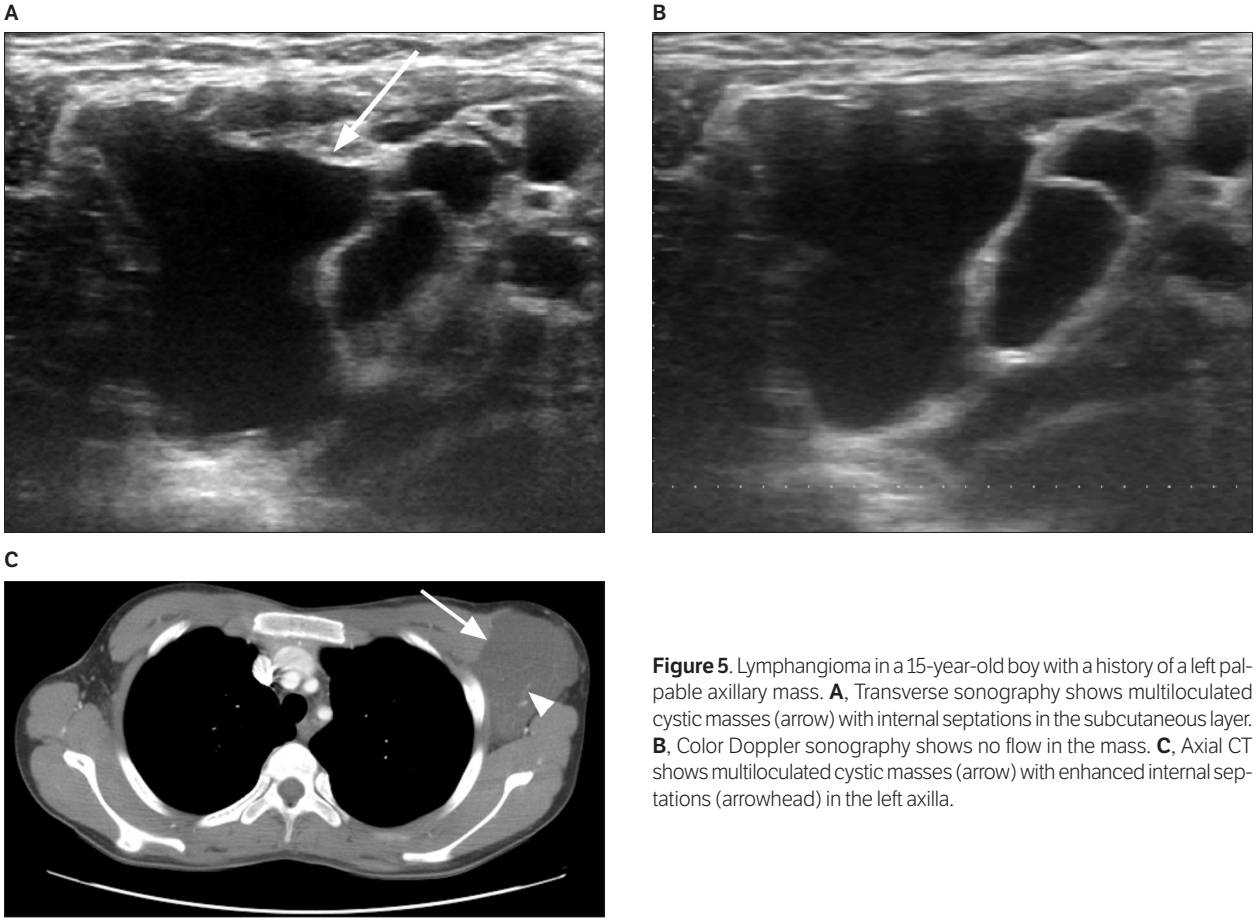

Figure 5. Lymphangioma in a 15-year-old boy with a history of a left palpable axillary mass. **A**, Transverse sonography shows multiloculated cystic masses (arrow) with internal septations in the subcutaneous layer. **B**, Color Doppler sonography shows no flow in the mass. **C**, Axial CT shows multiloculated cystic masses (arrow) with enhanced internal septations (arrowhead) in the left axilla.

resonance imaging shows well-margined masses with a high signal intensity on T2-weighted images and variable enhancement depending on the degree of fibrosis within the mass.[31] Computed tomography shows well-demarcated round, ovoid, or smoothly lobulated masses. Computed tomography is typically not used to evaluate breast and axillary masses in children and young women.[29]

Schwannomas

Schwannomas are benign nerve sheath tumors derived from Schwann cells, which normally produce the insulating myelin sheath covering peripheral nerves. They are the most common peripheral nerve tumors.[6] Schwannomas affect mainly the head, neck, and extremities. Axillary schwannomas are extremely uncommon.[32]

Sonography shows a well-demarcated heterogeneous hypoechoic oval mass. The coarse echo texture is considered to represent the portion of collagen deposition.[4,32] Other typical findings of large schwannomas are hyperechoic calcifications and internal degenerative cystic foci.[33] An echogenic ring within the mass is rare but is a pathognomonic feature of a schwannoma when present. In addition, tapering at the edges representing a mass in contiguity with the nerve and neurovascular bundle adjacent to the mass is an important feature (Figure 7A), and the reported frequency of contiguity with the involved nerve is 92%.[34] Some studies reported increased vascularity in schwannomas,[33,35] and Reynolds et al[34] reported that 50% of schwannomas showed increased vascularity with prominent arterial flow, but sometimes, no vascularity can be detected (Figure 7B).[32] Magnetic resonance imaging reveals homogeneous isointense masses relative to skeletal muscle on T1-weighted images,[33,34] whereas T2-weighted images reveal hyperintense masses with strong enhancement (Figure 7C).[32] Schwannomas in the breast usually appear as nonspecific well-defined round or oval masses on mammography.[36] Immunostaining for S100 protein shows strong staining of the spindle cells, characteristic of a schwannoma.[37]

Malignant Tumorous Conditions

Malignant Neuroendocrine Tumors

Malignant neuroendocrine tumors originate from cells of the endocrine and nervous systems throughout the body. The overall prevalence is estimated to be 1 to 2 cases per 100,000 people.[38] The most common sites of malignant neuroendocrine tumors are the appendix, rectum, ileum, and bronchi.[39] Neuroendocrine carcinomas can develop at any site in the body; however, they very rarely arise from soft tissue.[38,40]

On sonography, malignant neuroendocrine tumors are present as lobulated heterogeneous hypoechoic masses with increased vascularity (Figure 8, A and B).[38] Imaging using iodine I 123 metaiodobenzylguanidine demonstrates sensitivity and specificity of approximately 60% for identifying neuroendocrine tumors.[41] Neuroendocrine tumors are seen as lobulated circumscribed high-density masses on mammography (Figure 8C).[38] Histologically, neuroendocrine tumors form nests or sheets consisting of a uniform population of cells with an abundant eosinophilic cytoplasm and round nuclei (Figure 8D).[38]

Figure 6. Fibroadenoma in a 26-year-old woman with a history of a left palpable axillary mass. **A**, Transverse sonography shows a homogeneous hypoechoic lesion with a well-circumscribed mass in the subcutaneous layer (arrow). **B**, Color Doppler sonography shows increased blood flow (arrows) in the periphery of the fibroadenoma.

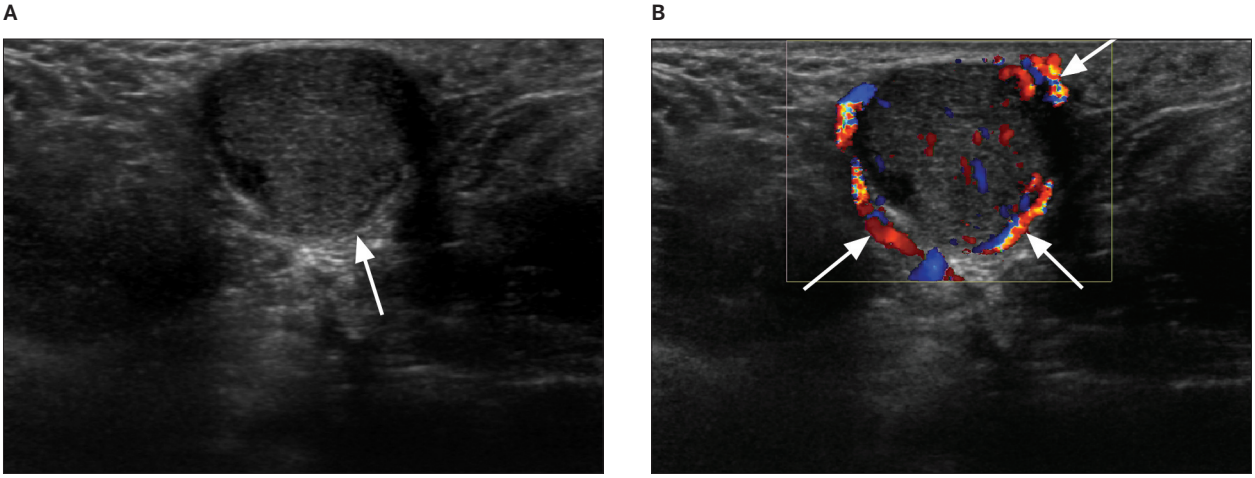

Lymph Node–Associated Diseases

Lymphomas are present as solid tumors of lymphoid cells and are common causes of superficial lymph node enlargement.[42] Most lymphomas are nodal or confluent nodal masses. The nodal or confluent nodal type means that lymphoma cells have infiltrated the lymph node, enlarging the node.[43] Lymphoma is usually a systemic disease, and a solitary lesion is unusual.[6]

Sonography shows that most soft tissue lymphomas are homogeneous, hypoechoic, and poorly defined.[43,44] They also have variable-size nodal or lobulating masses and frequently infiltrative margins, which are related to the fact that lymphoma cells easily invade surrounding tissue (Figure 9A).[45,46]

In addition, lymphomas have coarse internal echogenicity and are seen as hypoechoic masses with eccentric cortical thickening. Color Doppler imaging shows increased vascularity in both the periphery and center of enlarged lymph nodes.[6,47] Color Doppler imaging is useful for differential diagnosis between lymphomas and lymphadenitis. A single vascular pole with linear and regular branches is a sign of benignity, whereas multiple peripheral poles with distortion and displacement of the internal vessels indicate malignancy.[42] Mammography shows a well-circumscribed irregular uncalcified hyperdense oval mass in the axillary area (Figure 9B).[46–48] Computed tomography shows a large heterogeneous soft tissue mass in the right axilla (Figure 9C).[46] Histologically, lymphomas show diffuse replacement of the nodal architecture with malignant lymphoid cells.[6]

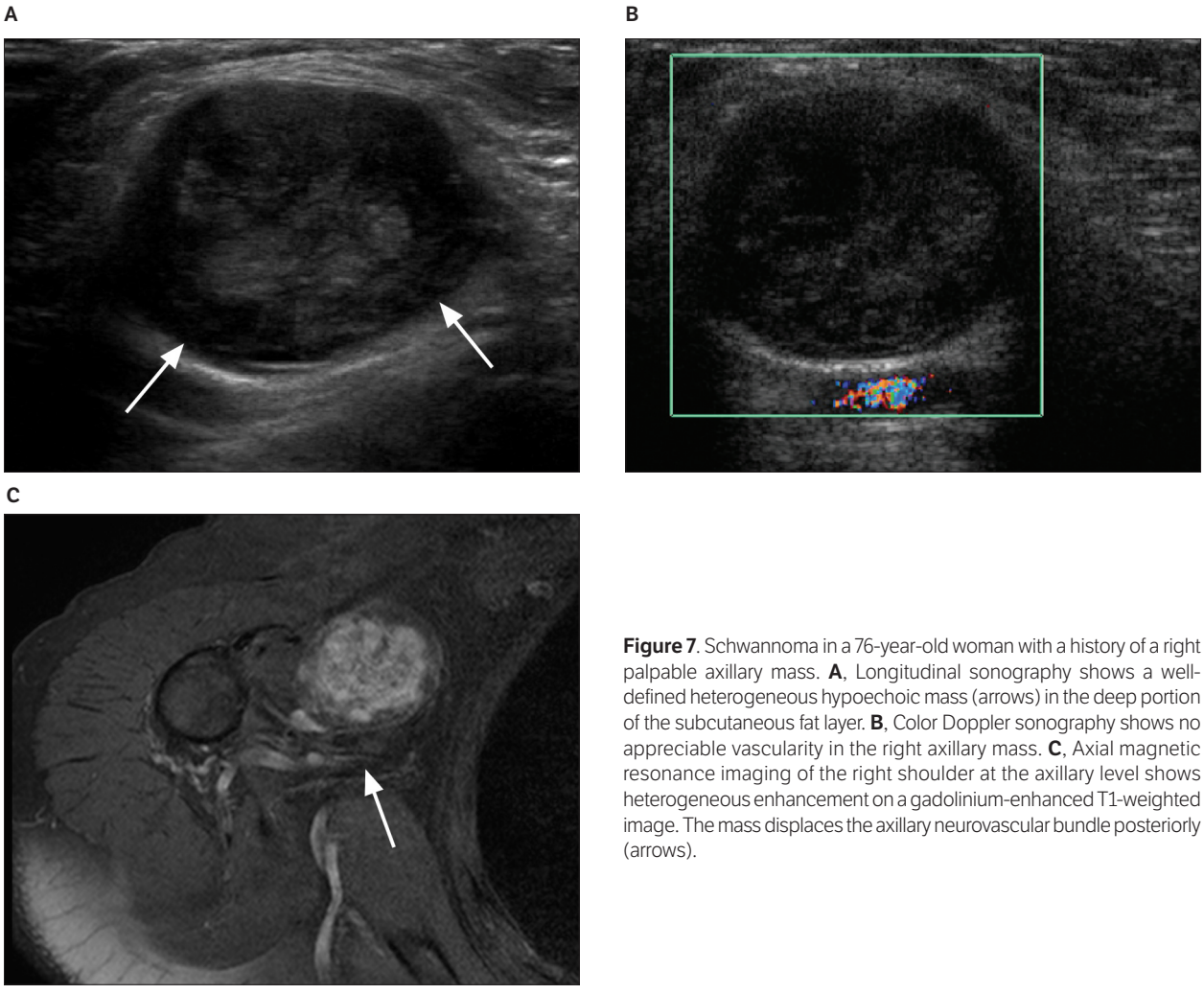

Figure 7. Schwannoma in a 76-year-old woman with a history of a right palpable axillary mass. **A**, Longitudinal sonography shows a well-defined heterogeneous hypoechoic mass (arrows) in the deep portion of the subcutaneous fat layer. **B**, Color Doppler sonography shows no appreciable vascularity in the right axillary mass. **C**, Axial magnetic resonance imaging of the right shoulder at the axillary level shows heterogeneous enhancement on a gadolinium-enhanced T1-weighted image. The mass displaces the axillary neurovascular bundle posteriorly (arrows).

Many cancers, including breast cancer, lung cancer, thyroid cancer, and, rarely ovarian cancer, can spread to the axillary lymph nodes.[49–52] In breast cancer, the axillary lymph node status is important because it is a prognostic indicator for patients' outcomes.[53] Sonography shows metastatic axillary lymph nodes that appear round rather than having the normal lentiform shape, hypoechogenicity of the cortex, asymmetric cortical thickening (>3 mm), and absence of the fatty hilum or eccentric hilum (Figure 10A).[54–56] In addition, nonhilar blood flow may be an additional indication of metastasis, probably because of engorgement of the cortical vascular network, owing to a disruption of the hilar blood flow that results from infiltration by metastases.[56] Alvarez et al[57] suggested that axillary sonography is moderately sensitive and fairly specific for diagnosis of axillary metastases. Sonographically guided biopsy of suspicious nodes increases the specificity, which reaches 100%.[57] Mammography shows enlarged dense nodes with well-defined borders (Figure 10B) and intranodal macrocalcifications.[57] Computed tomography shows multiple nodes with lobulated contours (Figure 10C).

Figure 8. Neuroendocrine tumors in a 69-year-old woman with a history of a right palpable axillary mass. **A**, Transverse sonography shows a large well-defined heterogeneous hypoechoic mass (arrow) in the subcutaneous layer. **B**, Power Doppler sonography shows mildly increased vascularity in multiple nodules (arrows) next to vessels (arrowheads). **C**, Mediolateral oblique mammography shows a well-defined hyperdense mass (arrow) in the right axilla. There is another hyperdense nodule adjacent to the main mass (arrowhead). **D**, Photomicrograph shows a tumor with rosette formation, cells with a finely granular cytoplasm, and oval to round nuclei with stippled chromatin and conspicuous nucleoli (hematoxylin-eosin, original magnification ×400).

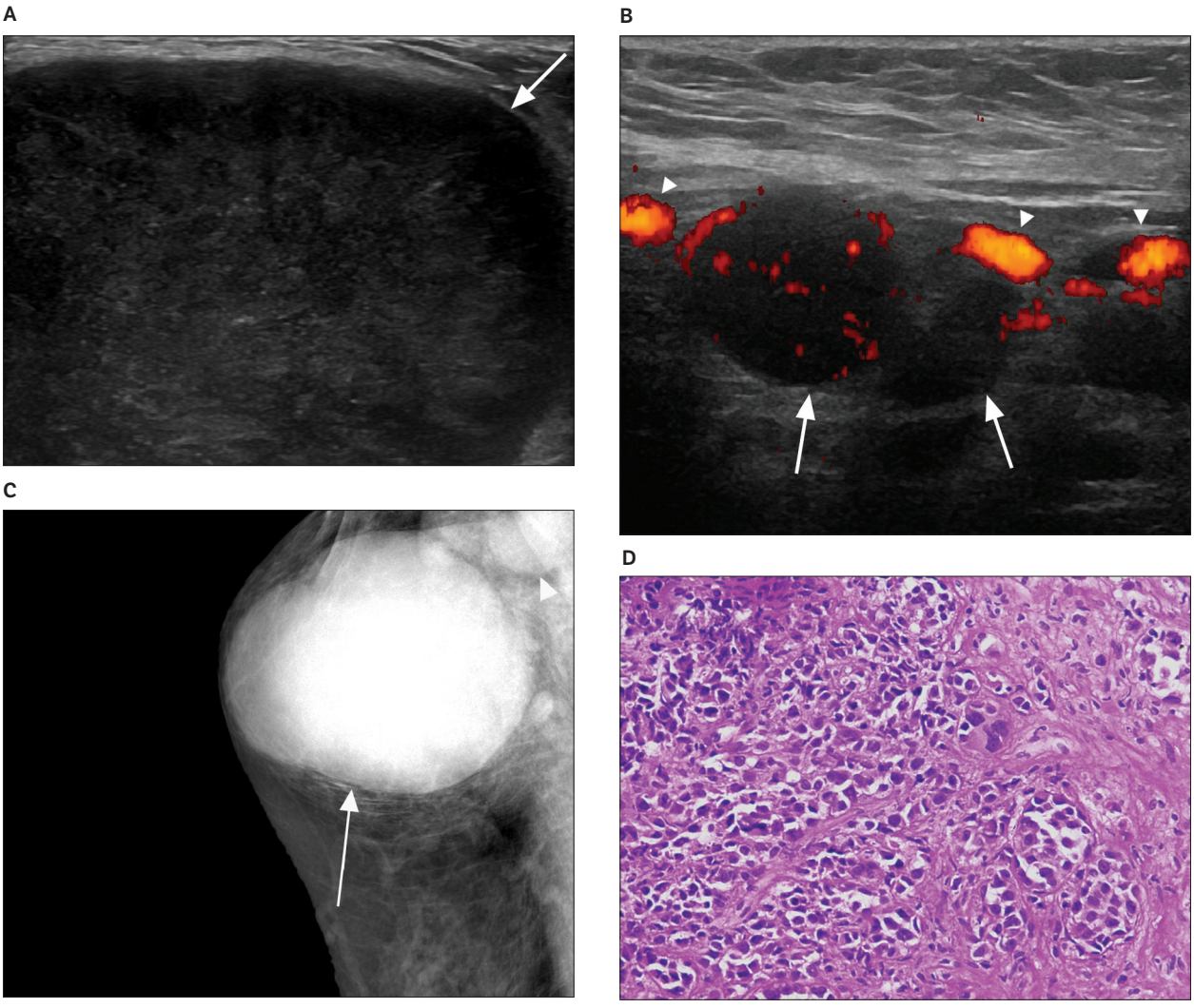

Figure 9. Lymphoma in a 55-year-old man with a history of a right palpable axillary mass. **A**, Transverse sonography shows a large hypoechoic mass with a lobulated contour (arrow) in the subcutaneous layer. **B**, Mediolateral oblique mammography shows a large hyperdense oval mass (arrows) in the right axilla. A BB (arrowhead) marks the site of the palpable abnormality. **C**, Axial CT shows a large soft tissue mass in the right axilla (arrow). Histologic examination confirmed that it was a large B-cell lymphoma.

A

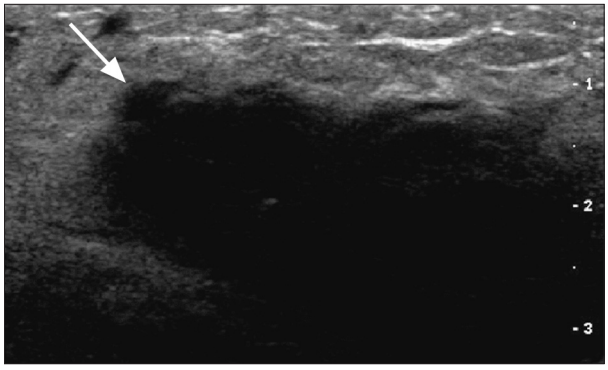

B

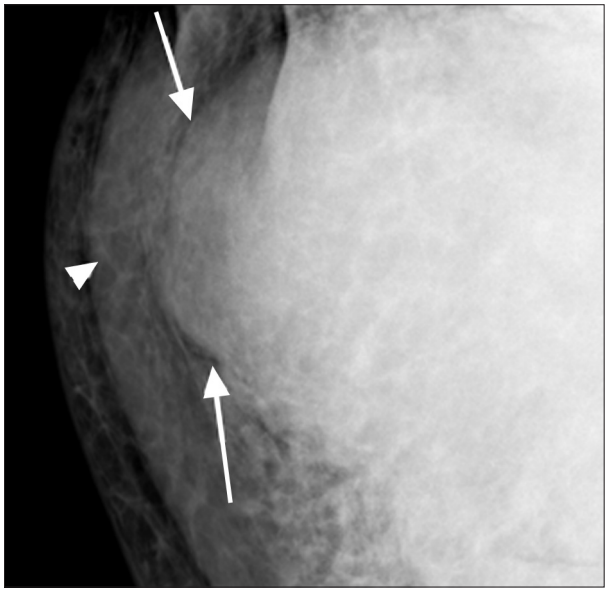

C

Figure 10. Axillary lymph node metastasis from breast cancer in a 68-year-old woman with a history of a left palpable axillary mass. **A**, Transverse sonography shows a hypoechoic oval lymph node with absence of the fatty hilum (arrows) in the subcutaneous layer. **B**, Mediolateral oblique mammography shows axillary lymph nodes that appear as well-circumscribed enlarged hyperdense masses in the left axilla (arrows). **C**, Axial CT shows multiple enlarged lymph nodes in the left axilla.

A

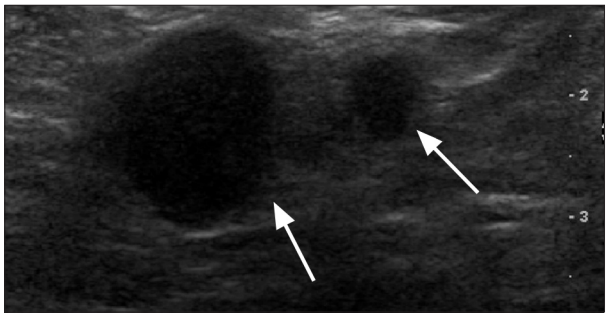

B

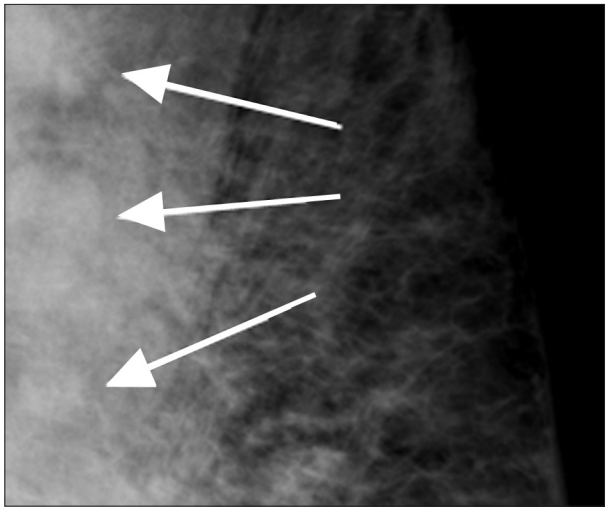

C

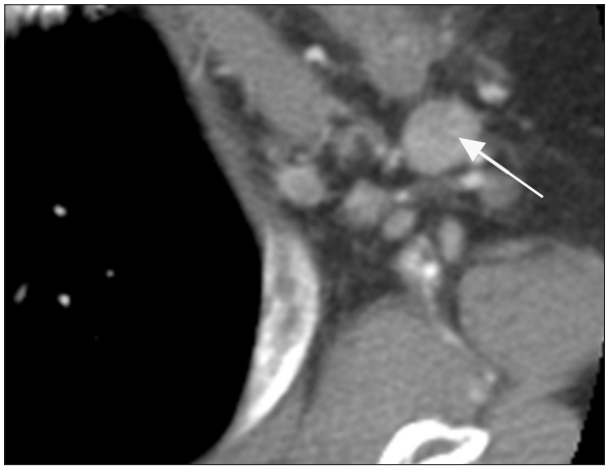

Conclusions

Axillary masses are not uncommon clinical findings. Many different pathologic conditions are present and diverse, ranging from benign to malignant. Various imaging modalities are available for evaluation of axillary masses, but sonography is the best choice because it is readily available and free of harmful radiation, and it can be used to guide diagnostic and therapeutic procedures. Knowledge of the sonographic findings of various axillary tumors can be helpful for the differential diagnosis of axillary masses.

References

1. Fishman EK, Zinreich ES, Jacobs CG, Rostock RA, Siegelman SS. CT of the axilla: normal anatomy and pathology. *Radiographics* 1986; 6:475–502.
2. Gakwaya A, Galukande M, Luwaga A, et al. Breast cancer guidelines for Uganda (2nd edition 2008). *Afr Health Sci* 2008; 8:126–132.
3. Yang WT, Suen M, Metreweli C. Mammographic, sonographic and histopathological correlation of benign axillary masses. *Clin Radiol* 1997; 52:130–135.
4. Kim EY, Ko EY, Han BK, et al. Sonography of axillary masses: what should be considered other than the lymph nodes? *J Ultrasound Med* 2009; 28:923–939.
5. Kim HS, Cha ES, Kim HH, Yoo JY. Spectrum of sonographic findings in superficial breast masses. *J Ultrasound Med* 2005; 24:663–680.
6. An JK, Oh KK, Jung WH. Soft-tissue axillary masses (excluding metastases from breast cancer): sonographic appearances and correlative imaging. *J Clin Ultrasound* 2005; 33:288–297.
7. Greer KE. Accessory axillary breast tissue. *Arch Dermatol* 1974; 109:88–89.
8. Ciralik H, Bulbuloglu E, Arican O, Citil R. Fibroadenoma of the ectopic breast of the axilla: a case report. *Pol J Pathol* 2006; 57:209–211.
9. Elmore SA. Histopathology of the lymph nodes. *Toxicol Pathol* 2006; 34:425–454.
10. Mukhopadhyay S, Farver CF, Vaszar LT, et al. Causes of pulmonary granulomas: a retrospective study of 500 cases from seven countries. *J Clin Pathol* 2012; 65:51–57.
11. Myhre-Jensen O. A consecutive 7-year series of 1331 benign soft tissue tumours. Clinicopathologic data: comparison with sarcomas. *Acta Orthop Scand* 1981; 52:287–293.
12. Lee JY, Kim SM, Fessell DP, Jacobson JA. Sonography of benign palpable masses of the elbow. *J Ultrasound Med* 2011; 30:1113–1119.
13. Copcu E, Sivrioglu N, Culhaci N. Axillary giant lipoma. *Plast Reconstr Surg* 2004; 114:1982–1983.
14. Gaskin CM, Helms CA. Lipomas, lipoma variants, and well-differentiated liposarcomas (atypical lipomas): results of MRI evaluations of 126 consecutive fatty masses. *AJR Am J Roentgenol* 2004; 182:733–739.
15. Ahuja AT, King AD, Kew J, King W, Metreweli C. Head and neck lipomas: sonographic appearance. *AJNR Am J Neuroradiol* 1998; 19:505–508.
16. Murphey MD, Carroll JF, Flemming DJ, Pope TL, Gannon FH, Kransdorf MJ. From the archives of the AFIP: benign musculoskeletal lipomatous lesions. *Radiographics* 2004; 24:1433–1466.
17. Inampudi P, Jacobson JA, Fessell DP, et al. Soft-tissue lipomas: accuracy of sonography in diagnosis with pathologic correlation. *Radiology* 2004; 233:763–767.
18. Bhatia KS, Rasalkar DD, Lee YP, et al. Real-time qualitative ultrasound elastography of miscellaneous non-nodal neck masses: applications and limitations. *Ultrasound Med Biol* 2010; 36:1644–1652.
19. Hong SH, Chung HW, Choi JY, Koh YH, Choi JA, Kang HS. MRI findings of subcutaneous epidermal cysts: emphasis on the presence of rupture. *AJR Am J Roentgenol* 2006; 186:961–966.
20. Yang WT, Whitman GJ, Tse GMK. Extratesticular epidermal cyst of the scrotum. *AJR Am J Roentgenol* 2004; 183:1084.
21. Huang CC, Ko SF, Huang HY, et al. Epidermal cysts in the superficial soft tissue: sonographic features with an emphasis on the pseudotestis pattern. *J Ultrasound Med* 2011; 30:11–17.
22. Farrer A, Forman W, Boike A. Epidermal inclusion cysts following minimal incision surgery. *J Am Podiatr Med Assoc* 1992; 82:537–541.
23. Jin W, Ryu KN, Kim GY, Kim HC, Lee JH, Park JS. Sonographic findings of ruptured epidermal inclusion cysts in superficial soft tissue: emphasis on shapes, pericystic changes, and pericystic vascularity. *J Ultrasound Med* 2008; 27:171–176.
24. Wortsman X. Common applications of dermatologic sonography. *J Ultrasound Med* 2012; 31:97–111.
25. Lee HS, Joo KB, Song HT, et al. Relationship between sonographic and pathologic findings in epidermal inclusion cysts. *J Clin Ultrasound* 2001; 29:374–383.
26. Whang IY, Lee J, Kim JS, Kim KT, Shin OR. Ruptured epidermal inclusion cysts in the subareolar area: sonographic findings in two cases. *Korean J Radiol* 2007; 8:356–359.
27. Youk JH, Kim EK, Kim MJ, Oh KK. Imaging findings of chest wall lesions on breast sonography. *J Ultrasound Med* 2008; 27:125–138.
28. Akaike G, Nozaki T, Makidono A, Saida Y, Hirabayashi T, Suzuki K. A case of lymphatic malformation/lymphangioma of the scrotum. *Acta Radiol Short Rep* 2012; 1:14.
29. Chung EM, Cube R, Hall GJ, González C, Stocker JT, Glassman LM. Breast masses in children and adolescents: radiologic-pathologic correlation. *Radiographics* 2009; 29:907–931.
30. Goel NB, Knight TE, Pandey S, Riddick-Young M, de Paredes ES, Trivedi A. Fibrous lesions of the breast: imaging-pathologic correlation. *Radiographics* 2005; 25:1547–1559.
31. Kuhl CK. MRI of breast tumors. *Eur Radiol* 2000; 10:46–58.
32. Sohn YM, Kim SY, Kim EK. Sonographic appearance of a schwannoma mimicking an axillary lymphadenopathy. *J Clin Ultrasound* 2011; 39:477–479.
33. Jin W, Kim GY, Park SY, et al. The spectrum of vascularized superficial soft-tissue tumors on sonography with a histopathologic correlation, part 1: benign tumors. *AJR Am J Roentgenol* 2010; 195:439–445.

34. Reynolds DL, Jacobson JA, Inampudi P, Jamadar DA, Ebrahim FS, Hayes CW. Sonographic characteristics of peripheral nerve sheath tumors. *AJR Am J Roentgenol* 2004; 182:741–744.
35. Belli P, Costantini M, Mirk P, Maresca G, Priolo F, Marano P. Role of color Doppler sonography in the assessment of musculoskeletal soft tissue masses. *J Ultrasound Med* 2000; 19:823–830.
36. Dialani V, Hines N, Wang Y, Slanetz P. Breast schwannoma. *Case Rep Med* 2011; 2011:930841.
37. Levy AD, Quiles AM, Miettinen M, Sobin LH. Gastrointestinal schwannomas: CT features with clinicopathologic correlation. *AJR Am J Roentgenol* 2005; 184:797–802.
38. Ogawa H, Nishio A, Satake H, et al. Neuroendocrine tumor in the breast. *Radiat Med* 2008; 26:28–32.
39. Kulke MH, Mayer RJ. Carcinoid tumors. *N Engl J Med* 1999; 340:858–868.
40. Hyer SL, McAleese J, Harmer CL. Neuroendocrine carcinoma arising in soft tissue: three case reports and literature review. *World J Surg Oncol* 2007; 5:77.
41. Kaltsas GA, Putignano P, Mukherjee JJ, et al. Carcinoid tumours presenting as breast cancer: the utility of radionuclide imaging with 123I-MIBG and 111In-DTPA pentetreotide. *Clin Endocrinol (Oxf)* 1998; 49:685–689.
42. Giovagnorio F, Galluzzo M, Andreoli C, De Cicco ML, David V. Color Doppler sonography in the evaluation of superficial lymphomatous lymph nodes. *J Ultrasound Med* 2002; 21:403–408.
43. Chiou HJ, Chou YH, Chiou SY, et al. Superficial soft-tissue lymphoma: sonographic appearance and early survival. *Ultrasound Med Biol* 2006; 32:1287–1297.
44. Cheng JW, Tang SF, Yu TY, Chou SW, Wong AM, Tsai WC. Sonographic features of soft tissue tumors in the hand and forearm. *Chang Gung Med J* 2007; 30:547–554.
45. Chiou HJ, Chou YH, Chiou SY, et al. High-resolution ultrasonography of primary peripheral soft tissue lymphoma. *J Ultrasound Med* 2005; 24:77–86.
46. Esserman L, Sexton R, Yu QQ, Cabello-Inchausti B. Mammographic, sonographic, and pathologic characteristics of Burkitt's lymphoma in a patient referred for diagnostic mammography. *AJR Am J Roentgenol* 2006; 186:1029–1032.
47. Sabate JM, Gomez A, Torrubia S, et al. Lymphoma of the breast: clinical and radiologic features with pathologic correlation in 28 patients. *Breast J* 2002; 8:294–304.
48. Feder JM, de Paredes ES, Hogge JP, Wilken JJ. Unusual breast lesions: radiologic-pathologic correlation. *Radiographics* 1999; 19(special issue):S11–S26.
49. Baruah BP, Goyal A, Young P, Douglas-Jones AG, Mansel RE. Axillary node staging by ultrasonography and fine-needle aspiration cytology in patients with breast cancer. *Br J Surg* 2010; 97:680–683.
50. Satoh H, Ishikawa H, Kagohashi K, Kurishima K, Sekizawa K. Axillary lymph node metastasis in lung cancer. *Med Oncol* 2009; 26:147–150.
51. Nakayama H, Wada N, Masudo Y, Rino Y. Axillary lymph node metastasis from papillary thyroid carcinoma: report of a case. *Surg Today* 2007; 37:311–315.
52. Ceccarelli F, Barberi S, Pontesilli A, Zancla S, Ranieri E. Ovarian carcinoma presenting with axillary lymph node metastasis: a case report. *Eur J Gynaecol Oncol* 2011; 32:237–239.
53. Fitzgibbons PL, Page DL, Weaver D, et al. Prognostic factors in breast cancer. College of American Pathologists Consensus Statement 1999. *Arch Pathol Lab Med* 2000; 124:966–978.
54. Kvistad KA, Rydland J, Smethurst HB, Lundgren S, Fjøsne HE, Haraldseth O. Axillary lymph node metastases in breast cancer: preoperative detection with dynamic contrast-enhanced MRI. *Eur Radiol* 2000; 10:1464–1471.
55. Kelly AM, Dwamena B, Cronin P, Carlos RC. Breast cancer sentinel node identification and classification after neoadjuvant chemotherapy: systematic review and meta analysis. *Acad Radiol* 2009; 16:551–563.
56. Abe H, Schmidt RA, Sennett CA, Shimauchi A, Newstead GM. US-guided core needle biopsy of axillary lymph nodes in patients with breast cancer: why and how to do it. *Radiographics* 2007; 27(special issue):S91–S99.
57. Alvarez S, Anorbe E, Alcorta P, Lopez F, Alonso I, Cortes J. Role of sonography in the diagnosis of axillary lymph node metastases in breast cancer: a systematic review. *AJR Am J Roentgenol* 2006; 186:1342–1348.